


ORIGINAL RESEARCH

Intravascular Imaging Findings After PCI in Patients With Focal and Diffuse Coronary Artery Disease

Hirofumi Ohashi , MD, PhD; Takuya Mizukami , MD, PhD; Jeroen Sonck , MD, PhD; Frederic Boussiet , MD; Brian Ko , MD, PhD; Bjarne L. Nørgaard , MD, PhD; Michael Mæng , MD, PhD; Jesper Møller Jensen, MD, PhD; Koshiro Sakai , MD, PhD; Hirohiko Ando , MD, PhD; Tetsuya Amano , MD, PhD; Nicolas Amabile , MD, PhD; Ziad Ali , MD, DPhil; Bernard De Bruyne , MD, PhD; Bon-Kwon Koo , MD, PhD; Hiromasa Otake, MD, PhD; Carlos Collet , MD, PhD

BACKGROUND: Following percutaneous coronary intervention (PCI), optical coherence tomography provides prognosis information. The pullback pressure gradient is a novel index that discriminates focal from diffuse coronary artery disease based on fractional flow reserve pullbacks. We sought to investigate the association between coronary artery disease patterns, defined by coronary physiology, and optical coherence tomography after stent implantation in stable patients undergoing PCI.

METHODS AND RESULTS: This multicenter, prospective, single-arm study was conducted in 5 countries (NCT03782688). Subjects underwent motorized fractional flow reserve pullbacks evaluation followed by optical coherence tomography-guided PCI. Post-PCI optical coherence tomography minimum stent area, stent expansion, and the presence of suboptimal findings such as incomplete stent apposition, stent edge dissection, and irregular tissue protrusion were compared between patients with focal versus diffuse disease. Overall, 102 patients (105 vessels) were included. Fractional flow reserve before PCI was 0.65 ± 0.14 , pullback pressure gradient was 0.66 ± 0.14 , and post-PCI fractional flow reserve was 0.88 ± 0.06 . The mean minimum stent area was $5.69\pm 1.99\text{ mm}^2$ and was significantly larger in vessels with focal disease ($6.18\pm 2.12\text{ mm}^2$ versus $5.19\pm 1.72\text{ mm}^2$, $P=0.01$). After PCI, incomplete stent apposition, stent edge dissection, and irregular tissue protrusion were observed in 27.6%, 10.5%, and 51.4% of the cases, respectively. Vessels with focal disease at baseline had a lower prevalence of incomplete stent apposition (11.3% versus 44.2%, $P=0.002$) and more irregular tissue protrusion (69.8% versus 32.7%, $P<0.001$).

CONCLUSIONS: Baseline coronary pathophysiological patterns are associated with suboptimal imaging findings after PCI. Patients with focal disease had larger minimum stent area and a higher incidence of tissue protrusion, whereas stent malapposition was more frequent in patients with diffuse disease.

Key Words: coronary artery disease ■ fractional flow reserve ■ optical coherence tomography ■ pullback pressure gradient

The pattern of coronary artery disease (CAD) is a key factor in selecting the treatment strategy for patients being considered for revascularization. Percutaneous coronary intervention (PCI) is useful in relieving symptoms, particularly in patients with focal

CAD.¹ However, a significant number of patients still experience symptoms after PCI; this is mainly driven by the presence of diffuse disease.² Furthermore, there are distinct differences in plaque characteristics between focal and diffuse CAD. Atherosclerotic plaques

Correspondence to: Carlos Collet, MD, PhD, Cardiovascular Center, Onze-Lieve-Vrouweziekenhuis, Moorselbaan 164, 9300, Aalst, Belgium.
Email: carloscollet@gmail.com

This article was sent to Amgad Mentias, MD, Associate Editor, for review by expert referees, editorial decision, and final disposition.

Supplemental Material is available at <https://www.ahajournals.org/doi/suppl/10.1161/JAHA.123.032605>

For Sources of Funding and Disclosures, see page 11.

© 2024 The Authors. Published on behalf of the American Heart Association, Inc., by Wiley. This is an open access article under the terms of the [Creative Commons Attribution-NonCommercial-NoDerivs](https://creativecommons.org/licenses/by-nc-nd/4.0/) License, which permits use and distribution in any medium, provided the original work is properly cited, the use is non-commercial and no modifications or adaptations are made.

JAHA is available at: www.ahajournals.org/journal/jaha

CLINICAL PERSPECTIVE

What Is New?

- This study investigated the impact of coronary artery disease patterns, defined by the novel pullback pressure gradient (PPG), on post-percutaneous coronary intervention (PCI) optical coherence tomography findings in patients with stable coronary artery disease.
- Notably, patients with focal coronary artery disease, characterized by higher PPG values (focal disease), achieved larger minimal stent areas and had a higher incidence of irregular tissue protrusion, whereas those with diffuse coronary artery disease (lower PPG) exhibited more incomplete stent apposition.
- The findings suggest that PPG could serve as a predictive tool for identifying suboptimal intravascular imaging outcomes post-PCI.

What Are the Clinical Implications?

- These results underscore the growing significance of coronary physiology in guiding and optimizing PCI procedures. Furthermore, they contribute to the body of evidence connecting vessel hemodynamics with plaque morphology and intravascular imaging outcomes following PCI.
- This research provides valuable insights into the potential use of PPG in enhancing PCI planning and improving post-PCI outcomes, highlighting the need for additional investigations into its clinical applicability.

Nonstandard Abbreviations and Acronyms

FFR	fractional flow reserve
IP	irregular tissue protrusion
ISA	incomplete stent apposition
IVI	intravascular imaging
MSA	minimum stent area
PPG	pullback pressure gradient

in vessels with focal disease are predominantly lipidic, whereas calcifications are more common in vessels with diffuse pressure losses.³

Intravascular imaging with intravascular ultrasound or optical coherence tomography (OCT) helps to assess lesion characteristics and enhance stent implantation.⁴ Use of intravascular imaging (IVI) guidance for stent optimization has been linked to improved clinical outcomes compared with angiographic guidance alone.^{5–7} Nonetheless, despite IVI, a sizable proportion

of patients remain with suboptimal PCI findings.⁸ This is partly attributed to the underlying plaque phenotype. Furthermore, various OCT findings following stent implantation have been identified as independent predictors of stent failure.^{9–12}

The pullback pressure gradient (PPG) is a recently developed metric that quantifies CAD patterns as focal or diffuse based on coronary physiology. Significant focal pressure gradients are the hallmark of focal disease, whereas the absence of such gradients characterizes diffuse CAD.¹³ Due to the differential underlying plaque morphology, post-PCI OCT findings are expected to differ between patients with focal versus diffuse disease; however, this remains to be described. We sought to investigate the association between CAD patterns defined by coronary physiology and post-PCI OCT findings in stable patients undergoing PCI.

METHODS

The data that support the findings of this study are available from the corresponding author upon reasonable request.

Study Population

This is a subanalysis of the P3 (Precise PCI Plan) study (NCT03782688). The P3 study was a multicenter, prospective, controlled, single-arm study conducted in 5 countries. The main results have been published elsewhere.¹⁴ Patients with stable CAD and invasive fractional flow reserve (FFR) ≤ 0.80 were eligible for inclusion. Patients underwent an invasive procedure with motorized intracoronary pressure recordings for longitudinal vessel evaluation followed by OCT. The P3 study validated a coronary computed tomography angiography-based revascularization planning tool in predicting post-PCI FFR. For this analysis, we included patients with pre-PCI FFR pullbacks and post-PCI OCT. The study protocol was approved by the institutional review board or ethics committee at each participating center. All patients signed informed consent before the study procedures.

The objective of the present study was to compare post-PCI OCT findings, namely, minimum stent area (MSA), stent underexpansion, stent edge dissection, irregular tissue protrusion (IP), and incomplete stent apposition (ISA) between patients with focal and diffuse CAD defined by PPG.

Invasive Procedure

Intracoronary nitroglycerin injection (100–200 μg) was administered before angiography. At least 2 projections separated by at least 30° were obtained. Coronary angiography was analyzed with 3-dimensional quantitative coronary angiography software (CAAS 8.2 software;

Pie Medical Imaging, Maastricht, the Netherlands). Pre-PCI FFR was performed with motorized pullbacks at a speed of 1 mm/s using a pullback device (Volcano R 100, San Diego, CA) during continuous adenosine infusion at 140 µg/kg per minute. Subsequently, OCT was performed to assess lesion characteristics and define the PCI strategy. All patients underwent PCI with the latest generation drug-eluting stents. Following PCI, OCT was performed to assess stent implantation. A final OCT pullback was required if an additional intervention was performed based on the OCT findings. Afterward, FFR with a motorized pullback was repeated. Thus, physiology and imaging were used for PCI optimization. Optimal procedural results were defined as MSA >5.5 mm² and post-PCI FFR >0.90.¹⁵ Cardiac biomarkers and an ECG were collected 6 to 24 hours after the procedure. To allow for comparison among different troponin assays, values were normalized to the assay-specific 99th percentile upper reference limit. Prognostically relevant major periprocedural myocardial injury was defined as post-PCI troponin >5×99th percentile upper reference limit. Periprocedural myocardial infarction was defined according to the fourth universal definition of myocardial infarction.^{16,17}

Physiological Assessment of CAD Patterns

From the FFR pullback curves, the PPG was calculated using a commercially available console (Coroflow version 3.5; Coroventis Research AP, Uppsala, Sweden). The PPG calculation has been described in detail elsewhere.¹³ Briefly, the PPG combines 2 parameters extracted from FFR pullback curves, namely, the maximal pressure gradient over 20% of the pullback and the extent of functional disease. The PPG values range from 0, indicating diffuse disease, to 1, pointing to focal CAD. This analysis used the median PPG value to define focal from diffuse CAD. After PCI, the residual PPG was calculated and was defined as the maximal residual pressure gradient (in FFR units) over 20% of the pullback. The quality of pressure tracings addressing the pressure tracings without a dicrotic notch, ventricularization, drift of >0.05 FFR units, unstable hyperemic conditions during the pullback maneuver, and pullback curves with major artifacts were adjudicated by a core laboratory.

OCT Assessment

A frequency domain ILUMIEN OPTIS system using a Dragonfly OPTIS Imaging Catheter (Abbott Vascular, St. Paul, MN) was used in the present study. An automated OCT pullback with a speed of 36 mm/s was performed during continuous intracoronary injection of 100% contrast medium, acquiring images at a rate of 180 frames/s. OCT was mandated before

and after stent implantation. Additional maneuvers for stent optimization based on OCT were left to the operator's discretion. OCT images were analyzed by the Core Laboratory using a dedicated offline review system (CAAS Intravascular version 2.1; Pie Medical Imaging) blinded to the angiographic data and clinical information. The quantitative measurements of cross-sectional OCT images were performed at 200-µm intervals throughout the stent and 5 mm proximally and distally. An automated algorithm defined minimal lumen area and MSA. Stent expansion was defined as the ratio between MSA and average reference lumen area. The mean stent area was calculated from the total stent volume divided by the entire stent length. ISA was defined as the separation of the inner surface of a stent strut from the inner vessel wall, in segments without a side branch, by a distance greater than or equal to the axial resolution of OCT plus the width of the stent strut of each stent type, including the polymer coating (>300 µm).¹⁰ IP was defined as material protrusion with an irregular surface into the lumen with a maximal height ≥100 µm. When thrombus could not be distinguished from IP, it was categorized as IP.¹⁰ Details of OCT definitions are shown in [Table S1](#).^{4,10,18–25}

Statistical Analysis

Variables are expressed as mean±SD and median (interquartile range [IQR]) for normally and nonnormally distributed data. Categorical variables are expressed as frequencies and percentages. Continuous variables were compared using the Student *t* test or Mann-Whitney tests, as appropriate, and categorical variables were compared using the χ^2 or Fisher exact test, as applicable. None of the *P* values were adjusted for multiple comparisons. Univariate and multivariable mixed-effects logistic regression analyses were used primarily for hypothesis testing, focusing on investigating the association between CAD patterns defined by the PPG and OCT findings after PCI. The univariate analysis incorporated clinical, procedural, and physiological characteristics based on their identified association with the outcomes.^{26–29} In multivariable analysis, 2 distinct models were developed for each outcome (ISA, stent edge dissection, IP, stent under-expansion). Although both models incorporated clinical covariates, Model 1 included PPG alongside age, hypertension, dyslipidemia, and renal function. Model 2 focused on plaque characteristics, adding variables such as calcified plaque and plaque rupture to the model.^{26–29} PPG and FFR were analyzed as continuous variables, with values increasing by 0.1 in univariate and multivariable mixed effects logistic regression analyses. Receiver operating characteristics curve analyses were used to assess the capacity of PPG

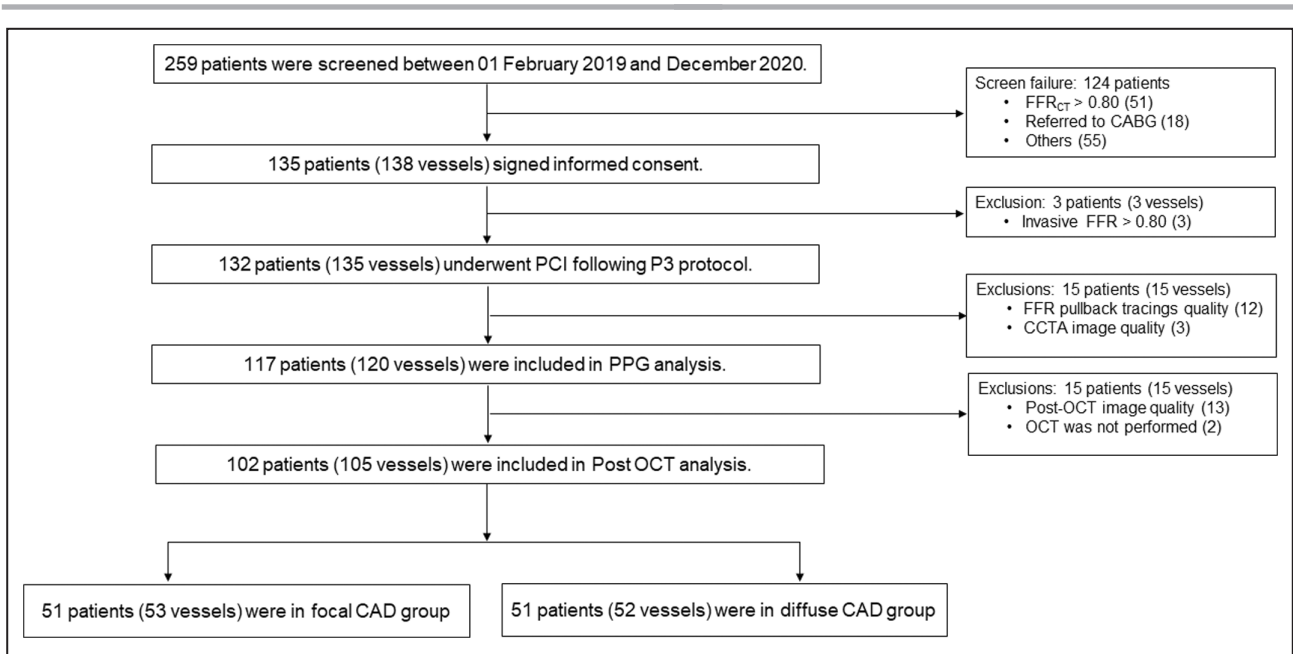


Figure 1. Study flowchart.

Focal CAD is defined as PPG ≥0.69 and diffuse CAD as PPG <0.69. CABG indicates coronary artery bypass grafting; CAD, coronary artery disease; CCTA, coronary computed tomography angiography; CT computed tomography; FFR, fractional flow reserve; OCT, optical coherence tomography; P3, Precise PCI Plan; PCI, percutaneous coronary intervention; and PPG, pullback pressure gradient.

for predicting adverse OCT findings. A *P* value ≤0.05 was considered to indicate statistical significance. All statistical analyses were performed using R statistical software (R Foundation for Statistical Computing, Vienna, Austria).

RESULTS

From February 2019 to December 2020, 259 patients were screened, and 102 patients (105 vessels) were included. The study flowchart is shown in [Figure 1](#).

Table 1. Baseline Clinical Characteristics

Variables	All	Focal CAD (PPG ≥0.69)	Diffuse CAD (PPG <0.69)	<i>P</i> value
No. of patients*	102	51	51	
Clinical characteristics				
Age, y, mean±SD	63.6±9.6	61.7±9.8	65.5±9.1	0.046
Sex (men), n (%)	80 (78.4)	40 (78.4)	40 (78.4)	1.00
BMI, mean±SD	27.0±3.4	27.1±3.4	27.0±3.4	0.94
Dyslipidemia, n (%)	83 (81.4)	39 (76.5)	44 (86.3)	0.31
Hypertension, n (%)	57 (55.9)	29 (56.9)	28 (54.9)	1.00
Diabetes, n (%)	24 (23.5)	11 (21.6)	13 (25.5)	0.82
Smoking, n (%)	21 (20.6)	11 (21.6)	10 (19.6)	1.00
Stroke, n (%)	3 (2.9)	2 (3.9)	1 (2.0)	1.00
Creatinine, mg/dL, mean±SD	0.94±0.20	0.94±0.23	0.94±0.17	0.90
LVEF, %, mean±SD	60.4±6.1	60.5±5.4	60.2±6.7	0.85
Clinical presentation, n (%)				0.03
Silent ischemia, n (%)	25 (24.5)	8 (15.7)	17 (33.3)	
CCS I, n (%)	34 (33.3)	14 (27.5)	20 (39.2)	
CCS II, n (%)	33 (32.4)	21 (41.2)	12 (23.5)	
CCS III, n (%)	8 (7.8)	6 (11.8)	2 (3.9)	
CCS IV, n (%)	2 (2.0)	2 (3.9)	0 (0.0)	

*Three patients had 2 vessels assessed. The lowest PPG was used to classify the patients as focal or diffuse CAD. BMI indicates body mass index; CAD, coronary artery disease; CCS, Canadian Cardiovascular Society; LVEF, left ventricular ejection fraction; and PPG, pullback pressure gradient.

Clinical characteristics stratified by CAD patterns are shown in Table 1. The mean age was 63.6±9.6 years and was lower in patients with focal CAD. Most patients were men, and 20% had diabetes without differences between groups. Clinical, lesion, and functional characteristics stratified by CAD patterns are shown in Table 2. The median PPG was 0.69 (IQR, 0.5–0.76). Diffuse disease was more frequently observed in the left anterior descending artery (LAD).

Procedural Characteristics

Procedural and post-PCI characteristics stratified by CAD patterns are shown in Table 3. Predilatation was more frequent in focal disease (64% versus 12%,

$P<0.001$), whereas postdilatation was performed in 90% of the cases without differences between vessels with focal or diffuse CAD. In patients with diffuse disease, the stent diameter was smaller (3.25 ± 0.85 mm versus 3.00 ± 0.37 mm, $P=0.049$), and the total stent length was longer (30.2 ± 12.7 mm versus 34.8 ± 11.3 mm, $P=0.053$) than in focal CAD. Post-PCI FFR and Δ FFR were significantly higher in focal CAD (0.90 ± 0.06 versus 0.85 ± 0.05 and 0.33 ± 0.14 versus 0.13 ± 0.08 , respectively).

Post-PCI OCT Stratified by CAD Patterns

Post-PCI OCT findings stratified by CAD patterns are shown in Table 4. After OCT-guided PCI, the mean MSA was 5.69 ± 1.99 mm² and was significantly larger

Table 2. Baseline Lesion Characteristics

Variables	All	Focal CAD (PPG ≥0.69)	Diffuse CAD (PPG <0.69)	P value
No. of vessels	105	53	52	
Vessels				
LAD, n (%)	77 (73.3)	27 (50.9)	50 (96.2)	<0.001
LCx, n (%)	12 (11.4)	11 (20.8)	1 (1.9)	
RCA, n (%)	16 (15.2)	15 (28.3)	1 (1.9)	
QCA				
Minimum lumen diameter, mm, median [IQR]	1.27 [1.01–1.55]	1.04 [0.86–1.31]	1.44 [1.26–1.67]	<0.001
Reference lumen diameter, mm, mean±SD	2.72±0.49	2.75±0.50	2.69±0.49	0.55
Minimum lumen area, mm ² , median [IQR]	1.27 [0.81–1.89]	0.85 [0.58–1.36]	1.62 [1.25–2.21]	<0.001
Mean reference lumen area, mm ² , mean±SD	6.01±2.24	6.14±2.25	5.88±2.23	0.56
Percent diameter stenosis, %, mean±SD	51.7±14.4	59.5±11.3	43.7±12.7	<0.001
Percent area stenosis, mean±SD	74.6±14.8	82.5±9.86	66.7±14.8	<0.001
Lesion length, mm, mean±SD	23.1±12.2	21.0±11.7	25.2±12.5	0.077
Physiology				
Resting Pd/Pa, mean±SD	0.82±0.14	0.76±0.14	0.88±0.06	<0.001
FFR, mean±SD	0.65±0.14	0.58±0.15	0.73±0.08	<0.001
Maximal pressure gradient, FFR, mean±SD	0.27±0.16	0.38±0.14	0.15±0.07	<0.001
Percent of disease, mean±SD	35±19	32±16	39±22	0.09
PPG, mean±SD	0.66±0.14	0.78±0.06	0.54±0.08	<0.001
Pre-PCI OCT				
No. of vessels*	61	18	43	
Minimum lumen area, mm ² , median [IQR]	1.51 [1.18–2.25]	1.17 [0.90–1.54]	1.76 [1.40–2.34]	0.02
Lesion length, mm, mean±SD	29.9±12.3	26.6±11.8	31.3±12.4	0.17
Fibrocalcific plaque, n (%)	33 (54.1)	6 (33.3)	27 (62.8)	0.07
Lipid-rich plaque, n (%)	36 (59.0)	13 (72.2)	23 (53.5)	0.28
Circumferential lipid-rich plaque, n (%)	8 (13.1)	7 (38.9)	1 (2.3)	0.001
Calcium plaque, n (%)	48 (78.7)	12 (66.7)	36 (83.7)	0.25
TCFA, n (%)	13 (21.3)	8 (44.4)	5 (11.6)	0.01
Fibrous cap thickness, mm, mean±SD	0.08±0.03	0.06±0.01	0.09±0.03	0.002
Plaque rupture, n (%)	16 (26.2)	7 (38.9)	9 (20.9)	0.26
Microchannel, n (%)	21 (34.4)	6 (33.3)	15 (34.9)	1.00
Macrophage, n (%)	15 (24.6)	5 (27.8)	10 (23.3)	0.96
Layered plaque, n (%)	39 (63.9)	14 (77.8)	25 (58.1)	0.24

CAD indicates coronary artery disease; FFR, fractional flow reserve; IQR, interquartile range; LAD, left anterior descending; LCx, left circumflex; OCT, optical coherence tomography; Pa, aortic pressure; PCI, percutaneous coronary intervention; Pd, distal coronary pressure; PPG, pullback pressure gradient; QCA, quantitative coronary angiography; RCA, right coronary artery; and TCFA, thin-cap fibroatheroma.

*Thirty-eight vessels were excluded due to predilatation, and 6 vessels were excluded due to pre-OCT image quality.

Table 3. Procedural Characteristics Stratified CAD Patterns

Variables	All	Focal CAD (PPG ≥ 0.69)	Diffuse CAD (PPG < 0.69)	P value
N	105	53	52	
Procedural characteristics				
Total stent length, mm, mean \pm SD	32.5 \pm 12.2	30.2 \pm 12.7	34.8 \pm 11.3	0.053
Mean stent diameter, mm, mean \pm SD	3.13 \pm 0.67	3.25 \pm 0.85	3.00 \pm 0.37	0.049
No. of stents, mean \pm SD	1.18 \pm 0.39	1.19 \pm 0.39	1.17 \pm 0.38	0.84
Predilatation, n (%)	93 (91.2)	48 (94.1)	45 (88.2)	0.487
Postdilatation, n (%)	94 (89.5)	46 (86.8)	48 (92.3)	0.55
Postdilatation balloon diameter, mm, mean \pm SD	3.52 \pm 0.53	3.60 \pm 0.49	3.45 \pm 0.57	0.069
Postdilatation balloon pressure, atm \pm SD	17.3 \pm 3.73	18.1 \pm 3.37	16.6 \pm 3.94	0.057
Post-PCI physiological assessment				
Pd/Pa, mean \pm SD	0.94 \pm 0.05	0.96 \pm 0.04	0.93 \pm 0.04	<0.001
FFR, mean \pm SD	0.88 \pm 0.06	0.90 \pm 0.06	0.85 \pm 0.05	<0.001
FFR >0.90, n (%)	35 (33.3)	29 (54.7)	6 (11.5)	<0.001
Functional gain FFR, mean \pm SD	0.23 \pm 0.15	0.33 \pm 0.14	0.13 \pm 0.08	<0.001
Residual PPG, mean \pm SD	0.05 \pm 0.03	0.05 \pm 0.03	0.06 \pm 0.03	0.019

CAD indicates coronary artery disease; FFR, fractional flow reserve; Pa, aortic pressure; PCI, percutaneous coronary intervention; Pd, distal coronary pressure; and PPG, pullback pressure gradient.

Table 4. Post-Percutaneous Coronary Intervention Suboptimal Optical Coherence Tomography Findings

Variables	All	Focal CAD (PPG ≥ 0.69)	Diffuse CAD (PPG < 0.69)	P value
No. of vessels	105	53	52	
Minimum stent area, mm ² , mean \pm SD	5.69 \pm 1.99	6.18 \pm 2.12	5.19 \pm 1.72	0.01
Stent expansion, %, mean \pm SD	81 \pm 19	81 \pm 14	81 \pm 19	0.97
Minimum stent area ≤ 5.5 mm ² , n (%)	63 (60.0)	25 (47.2)	38 (73.1)	0.01
Minimum stent area ≤ 4.5 mm ² , n (%)	30 (28.6)	12 (22.6)	18 (34.6)	0.25
Minimum stent area ≤ 3.5 mm ² , n (%)	8 (7.6)	2 (3.8)	6 (11.5)	0.26
Total stent volume, mm ³ , mean \pm SD	242.0 \pm 98.9	235.0 \pm 103.0	249.1 \pm 95.0	0.47
Mean stent area, mm ² , mean \pm SD	7.57 \pm 2.23	8.00 \pm 2.35	7.14 \pm 2.03	0.049
Malapposition, n (%)	40 (38.1)	12 (22.6)	28 (53.8)	0.002
Malapposition distance, μ m, mean \pm SD	409.0 \pm 184.2	343.3 \pm 151.0	437.1 \pm 192.4	0.14
Malapposition distance ≥ 300 μ m, n (%)	29 (27.6)	6 (11.3)	23 (44.2)	<0.001
Malapposition length, mm, mean \pm SD	2.50 \pm 1.27	2.41 \pm 1.58	2.54 \pm 1.14	0.51
Malapposition arc, $^{\circ}$, mean \pm SD	87.6 \pm 38.1	89.7 \pm 39.2	86.7 \pm 38.3	0.89
Any stent edge dissection, n (%)	11 (10.5)	3 (5.7)	8 (15.4)	0.19
Dissection proximal, n (%)	5 (6.0)	2 (3.8)	3 (5.8)	1.00
Dissection distal, n (%)	6 (5.8)	1 (1.9)	5 (9.6)	0.21
Dissection angle, mean \pm SD	37.8 \pm 37.4	24.3 \pm 26.0	42.8 \pm 41.3	0.41
Dissection length, mm, mean \pm SD	1.62 \pm 1.03	1.40 \pm 0.80	1.71 \pm 1.16	0.69
Dissection area, mm ² , mean \pm SD	1.62 \pm 1.99	0.85 \pm 0.49	1.95 \pm 2.33	0.45
Maximum circumferential extension, mm, mean \pm SD	0.88 \pm 0.70	0.70 \pm 0.43	0.96 \pm 0.81	0.62
Maximum axial extension, mm, mean \pm SD	0.40 \pm 0.25	0.46 \pm 0.14	0.37 \pm 0.28	0.62
Irregular tissue protrusion, n (%)	54 (51.4)	37 (69.8)	17 (32.7)	<0.001
Disrupted fibrous protrusion, n (%)	72 (68.6)	32 (60.4)	40 (76.9)	0.11

CAD indicates coronary artery disease; and PPG pullback pressure gradient.

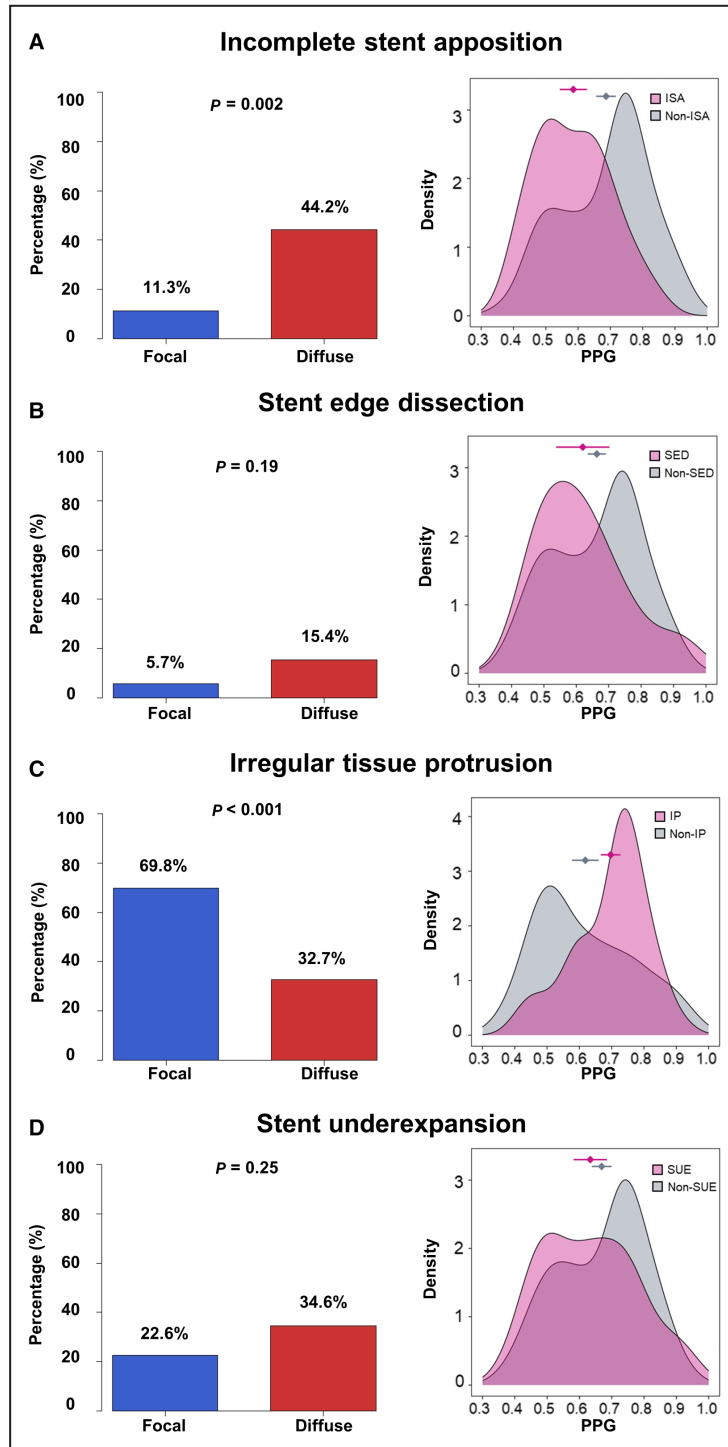


Figure 2. Comparison of the frequency of suboptimal OCT findings between focal and diffuse CAD.

The bar plots show the suboptimal OCT findings stratified CAD pattern defined by PPG. Focal CAD is depicted in blue, whereas diffuse disease is in red. **A**, Left shows the prevalence of ISA stratified by focal (blue bars) and diffuse disease (red bars). The right panel shows the PPG density curve stratified by the presence of ISA (purple) and absence of ISA (gray). **B**, Left shows the prevalence of SED stratified by focal (blue bars) and diffuse disease (red bars). The right panel shows the PPG density curve stratified by the presence of SED (purple) and absence of SED (gray). **C**, Left shows the prevalence of IP stratified by focal (blue bars) and diffuse disease (red bars). The right panel shows the PPG density curve stratified by the presence of IP (purple) and absence of IP (gray). **D**, Left shows the prevalence of stent underexpansion stratified by focal (blue bars) and diffuse disease (red bars). The right panel shows the PPG density curve stratified by the presence of stent underexpansion (purple) and absence of stent underexpansion (gray). CAD indicates coronary artery disease; IP, irregular tissue protrusion; ISA, incomplete stent apposition; OCT, optical coherence tomography; PPG, pullback pressure gradient; SED, stent edge dissection; and SUE, stent underexpansion.

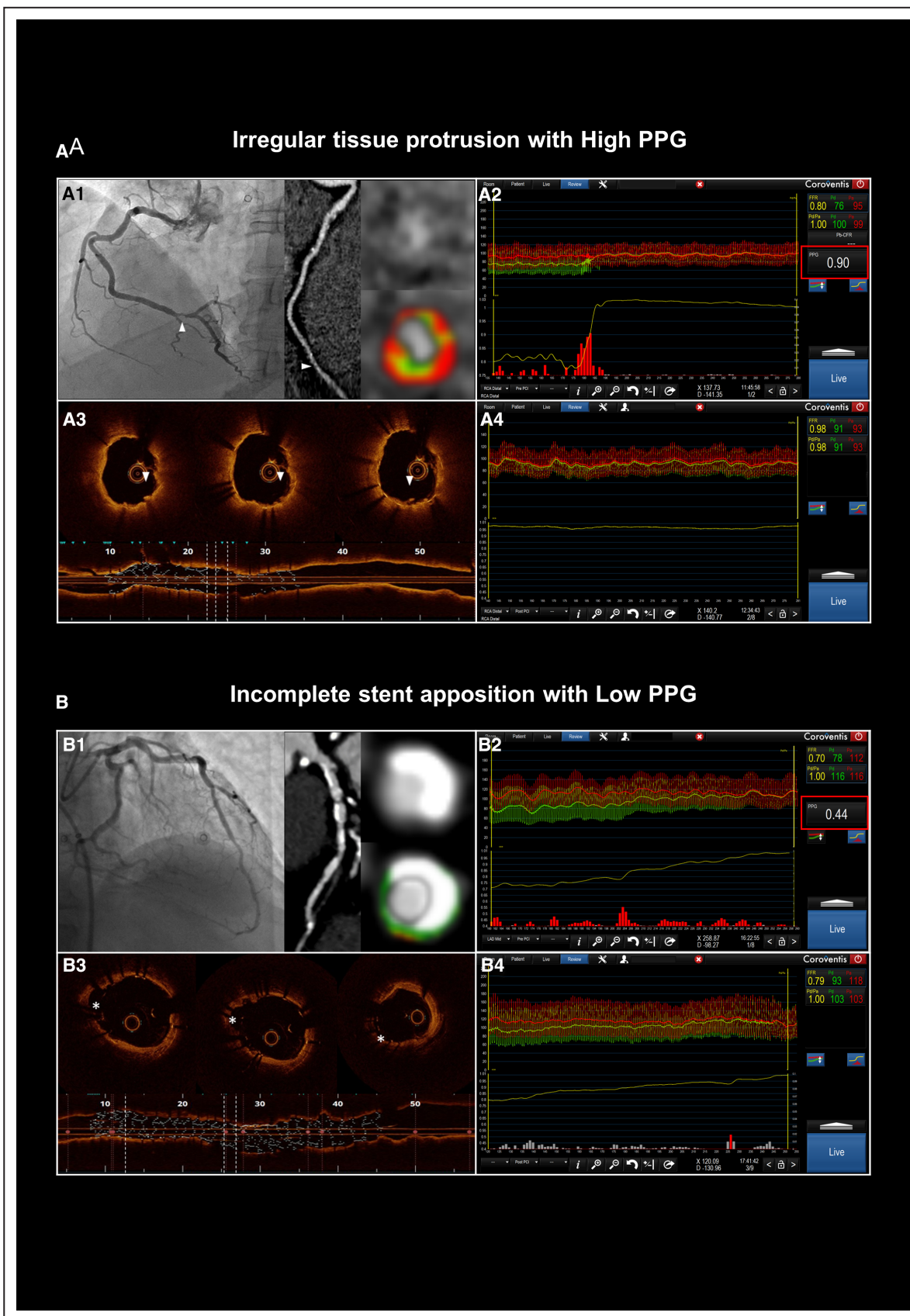


Figure 3. Representative cases of irregular tissue protrusion with a high PPG and incomplete stent apposition with a low PPG.

A, A case with focal CAD (high PPG). **B**, A patient with diffuse CAD (low PPG). A1 and B1 show coronary angiography (the white arrowheads identify the lesion), the CCTA straight multiplanar reconstructions of the vessel, and the cross-section with and without tissue characterization, respectively. A2 and B2 present the pre-PCI FFR pullback tracings with the corresponding FFR and PPG values. The red bars depict the location and magnitude of pressure drops along the coronary vessel. A3 and B3 show cross-sectional and longitudinal OCT images, respectively. The white arrowheads show irregular tissue protrusion, and the asterisks (*) depict incomplete stent apposition. A4 and B4 present the post-PCI FFR pullback tracings with the corresponding FFR values. CAD indicates coronary artery disease; CCTA, coronary computed tomography angiography; FFR, fractional flow reserve; OCT optical coherence tomography; PCI, percutaneous coronary intervention; and PPG pullback pressure gradient.

in patients with focal CAD ($6.18 \pm 2.12 \text{ mm}^2$ versus $5.19 \pm 1.72 \text{ mm}^2$, $P=0.01$). In the regression analysis, PPG was significantly associated with MSA (B coefficient, 0.38 [95% CI, 0.104–0.649]; $P=0.007$). There was no difference in stent expansion between vessels with focal and diffuse disease. ISA, stent edge dissection, IP, and stent underexpansion were observed in 27.6%, 10.5%, 51.4%, and 28.6%, respectively. ISA was more frequently observed in diffuse CAD (11.3% versus 44.2%, $P=0.002$), whereas IP was more prevalent in patients with focal CAD (69.8% versus 32.7%, $P<0.001$, Figure 2). PPG was independently associated with plaque rupture and calcium plaque (odds ratio [OR], 2.12 [95% CI, 1.50–3.13]; $P<0.001$ and OR, 0.52 [95% CI 0.335–0.77]; $P=0.002$, respectively). In addition, PPG was also associated with ISA and IP (Table S2). The predicted capacity of PPG to detect ISA showed an area under the curve of 0.72 (95% CI, 0.61–0.82) and 0.66 (95% CI, 0.55–0.77) for IP (Figure S1). Representative cases of focal and diffuse disease and post-PCI OCT findings are shown in Figure 3. Procedural outcomes in focal and diffuse disease are shown in Table S3.

DISCUSSION

This study compared intravascular imaging outcomes immediately after PCI in patients with focal versus diffuse disease defined by PPG. The main results can be summarized as follows: (1) PCI guided by IVI in vessels with focal disease resulted in larger MSA compared with vessels with diffuse disease. (2) IP was observed in the majority of the cases with focal disease, and it was more prevalent than in vessels with diffuse disease. (3) Stent malapposition was 2 times more common in vessels with diffuse disease than in focal CAD (Figure 4).

The present study increases our understanding of the impact of the baseline pathophysiological CAD pattern on morphological IVI findings following PCI. These results were obtained using PPG to standardize the diagnosis of focal versus diffuse disease before stenting. MSA, an independent predictor of stent failure, was significantly smaller in vessels with low PPG (diffuse disease).^{15,30} Interestingly, this was not driven

by vessel size, because reference vessel diameter was similar between vessels with focal or diffuse disease. It can be hypothesized that the association between diffuse hemodynamic disease and small MSA was partly mediated by the underlying plaque. Vessels with diffuse disease have been shown to have greater calcium arc and longer calcific plaques, which have been associated with small stent areas.^{3,31} It is crucial to acknowledge that the aforementioned findings were observed after IVI-guided PCI with high rates of stent postdilatation. The management of diffuse CAD remains a therapeutic challenge, and future clinical trials should address the optimal treatment strategy.

Irregular protrusion arises as a consequence of the lipid core penetrating through the stent struts and has been identified after PCI in lipid-rich lesions.³² In the current study, IP was observed in 50% of the patients, with a 2-fold higher prevalence in vessels exhibiting focal disease (high PPG). Importantly, IP has been identified as an independent predictor of target lesion revascularization, underscoring its clinical relevance.^{10,33,34} However, it must be recognized that despite the independent association between PPG and IP, the predicted capacity of PPG to detect IP was modest (area under the curve of 0.66). We also found that vessels with diffuse CAD (low PPG at baseline) had a higher prevalence of ISA after PCI. It is worth noting that ISA has been associated with late and very late stent thrombosis with the first-generation drug-eluting stents.³⁵ However, more contemporary studies involving second-generation drug-eluting stents have not found a significant association between ISA and adverse events.^{9,11} In addition to assessing the presence of stent malposition, the distance of incompletely apposed struts also appears to hold clinical relevance. Notably, larger malapposition distances (eg, $>300 \mu\text{m}$) result in flow strut disturbances and an increased risk of delayed strut coverage, with smaller distances of ISA facilitating a faster healing process, potentially enabling the safe discontinuation of double antiplatelet therapy.^{36,37} The potential benefit of prolonged double antiplatelet therapy in cases of diffuse disease requires further study. There is an ongoing debate on the association between ISA and adverse outcomes after PCI; the general consensus is that larger areas of malapposition should be addressed during the procedure.⁸

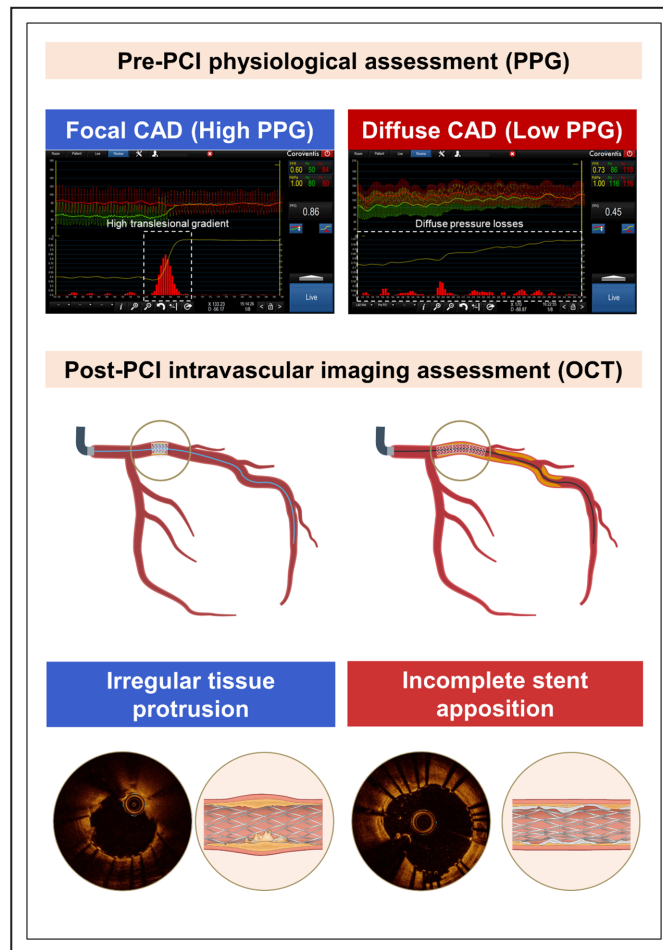


Figure 4. Summary of current study findings. CAD indicates coronary artery disease; OCT, optical coherence tomography; PCI, percutaneous coronary intervention; and PPG, pullback pressure gradient.

Finally, the proportion of edge dissections was 3 times higher in vessels with diffuse disease (15.5% in diffuse versus 5.7% in focal); nonetheless, this finding was not statistically different between focal and diffuse disease. These findings suggest a different underlying atherosclerotic substrate leading to suboptimal PCI outcomes that is identifiable using PPG. The long-term clinical impact of differential PCI outcomes between focal versus diffuse disease is being investigated in the PPG Global registry (NCT04789317).³⁸

There is growing interest in the use of coronary physiology to guide and optimize PCI. Moreover, there is increasing awareness of the clinical value of longitudinal vessel assessment with pressure pullback maneuvers to define the appropriateness of PCI and tailor treatment strategies. The present study adds to the body of evidence correlating vessel hemodynamics with plaque morphology and IVI outcomes after PCI. Furthermore, this study sheds light on the relationship between pre-PCI physiological assessment and the potential presence of

suboptimal OCT findings. Diffuse disease, as determined by coronary physiology, is associated with lower post-PCI FFR values, reduced Δ FFR, and the persistence of angina after PCI. This observation raises the hypothesis that pharmacological interventions may represent a more optimal therapeutic option for patients presenting with diffuse coronary disease. Consequently, there is a compelling rationale for the initiation of a clinical trial aimed at elucidating the potential advantages of a precision treatment approach, using PCI for patients with focal coronary disease and pharmacological therapy for those with diffuse coronary disease.

LIMITATIONS

This study has several limitations. First is the relatively small sample size. Nonetheless, this cohort was systematically studied with OCT and motorized FFR pullbacks, providing a unique opportunity to assess the link

between physiology and IVI findings after PCI. Second, baseline OCT was not available for all patients because of technical difficulties during image acquisition. Third, in the absence of a PPG cutoff, we used the median PPG value to define focal versus diffuse disease. To enhance the statistical validity of our findings, we have corroborated the results through division into tertiles (Table S4). A large-scale prospective study is ongoing to define the PPG cutoff. Fourth, we did not include pre-PCI OCT plaque characteristics regression analysis due to the high attrition rate related to the high frequency of predilatation hampering accurate plaque evaluation. Finally, the present study is focused on the association between coronary hemodynamic and post-OCT sub-optimal findings; the impact of these findings on clinical outcomes remains to be determined.

CONCLUSIONS

Post-PCI OCT findings correlate with baseline pathophysiological CAD patterns. PCI in vessels with focal disease at baseline (high PPG) resulted in larger MSA and had a higher prevalence of in-stent irregular tissue protrusion by OCT, whereas patients with diffuse disease (low PPG) had a higher prevalence ISA. PPG might be useful in predicting suboptimal intravascular imaging findings.

ARTICLE INFORMATION

Received September 10, 2023; accepted January 17, 2024.

Affiliations

Cardiovascular Center Aalst, OLV Clinic, Aalst, Belgium (H.O., T.M., J.S., F.B., K.S., B.D.B., C.C.); Department of Cardiology, Aichi Medical University, Aichi, Japan (H.O., H.A., T.A.); Division of Clinical Pharmacology, Department of Pharmacology, Showa University, Tokyo, Japan (T.M.); Department of Cardiovascular Medicine, Gifu Heart Center, Gifu, Japan (T.M.); Department of Cardiology, Toulouse University Hospital, Toulouse, France (F.B.); Monash Cardiovascular Research Centre, Monash University and Monash Heart, Monash Health, Clayton, Victoria, Australia (B.K.); Department of Cardiology, Aarhus University Hospital, Aarhus, Denmark (B.L.N., M.M., J.M.J.); Department of Medicine, Division of Cardiology, Showa University School of Medicine, Tokyo, Japan (K.S.); Department of Cardiology, Institut Mutualiste Montsouris, Paris, France (N.A.); DeMatteis Cardiovascular Institute, St. Francis Hospital & Heart Center, Roslyn, NY (Z.A.); Department of Cardiology, Lausanne University Hospital, Lausanne, Switzerland (B.D.B.); Department of Internal Medicine and Cardiovascular Center, Seoul National University Hospital, Seoul, South Korea (B-K.K.); and Division of Cardiovascular Medicine, Department of Internal Medicine, Kobe University Graduate School of Medicine, Kobe, Japan (H.O.).

Acknowledgments

We appreciate the support of the coinvestigators and study coordinators participating in the P3 study.

Sources of Funding

The study was sponsored by the Cardiac Research Institute Aalst with an unrestricted grant from HeartFlow Inc.

Disclosures

Dr Mizukami reports receiving consulting fees from Zeon Medical and HeartFlow Inc. and speaker fees from Abbott Vascular. Dr Bousset received consultancy fees from Boston Scientific, B-Braun, and Amgen. Dr Nørgaard

has received an unrestricted institutional research grant from HeartFlow Inc., outside of the submitted work. Dr Mæng is supported by a grant from the Novo Nordisk Foundation (grant number NNFOC0074083) and has received lecture and advisory board fees from Novo Nordisk, Denmark. Dr Amabile received proctoring and consulting fees for Abbott Vascular and Boston Scientific, consulting fees for Shockwave Medical, and institutional research grants from Abbott Vascular. Dr Ali received institutional grants from Abbott Vascular and Cardiovascular System Inc. to Columbia University and the Cardiovascular Research Foundation; honoraria from Amgen, Astra Zeneca, and Boston Scientific; and equity from Shockwave. Dr De Bruyne reports receiving consultancy fees from Boston Scientific and Abbott Vascular, research grants from Corovantis Research, Pie Medical Imaging, CathWorks, Boston Scientific, Siemens, HeartFlow Inc., and Abbott Vascular, and owner equity in Siemens, GE, Philips, HeartFlow Inc., Edwards Life Sciences, Bayer, Sanofi, and Celyad. Dr Koo received an institutional research grant from Abbott Vascular and Philips Volcanumber. Dr Otake received research funds from Abbott Medical Japan. Dr Collet reports receiving research grants from Biosensor, Corovantis Research, Medis Medical Imaging, Pie Medical Imaging, CathWorks, Boston Scientific, Siemens, HeartFlow Inc., Abbott Vascular, and consultancy fees from HeartFlow Inc., OpSens, Abbott Vascular, and Philips Volcano. The remaining authors have no disclosures to report.

Supplemental Material

Data S1.

REFERENCES

- Spertus JA, Jones PG, Maron DJ, O'Brien SM, Reynolds HR, Rosenberg Y, Stone GW, Harrell FE Jr, Boden WE, Weintraub WS, et al. Health-status outcomes with invasive or conservative care in coronary disease. *N Engl J Med*. 2020;382:1408–1419. doi: [10.1056/NEJMoa1916370](https://doi.org/10.1056/NEJMoa1916370)
- Collet C, Collison D, Mizukami T, McCartney P, Sonck J, Ford T, Munhoz D, Berry C, De Bruyne B, Oldroyd K. Differential improvement in angina and health-related quality of life after PCI in focal and diffuse coronary artery disease. *JACC Cardiovasc Interv*. 2022;15:2506–2518. doi: [10.1016/j.jcin.2022.09.048](https://doi.org/10.1016/j.jcin.2022.09.048)
- Sakai K, Mizukami T, Leipsic J, Belmonte M, Sonck J, Nørgaard BL, Otake H, Ko B, Koo BK, Maeng M, et al. Coronary atherosclerosis phenotypes in focal and diffuse disease. *JACC Cardiovasc Imaging*. 2023;81:1057. doi: [10.1016/j.jcmg.2023.05.018](https://doi.org/10.1016/j.jcmg.2023.05.018)
- Ali Z, Landmesser U, Karimi Galougahi K, Maehara A, Matsumura M, Shlofmitz RA, Guagliumi G, Price MJ, Hill JM, Akasaka T, et al. Optical coherence tomography-guided coronary stent implantation compared to angiography: a multicentre randomised trial in PCI - design and rationale of ILUMIEN IV: OPTIMAL PCI. *EuroIntervention*. 2021;16:1092–1099. doi: [10.4244/EIJ-D-20-00501](https://doi.org/10.4244/EIJ-D-20-00501)
- Buccheri S, Franchina G, Romano S, Puglisi S, Venuti G, D'Arrigo P, Francaviglia B, Scalia M, Condorelli A, Barbanti M, et al. Clinical outcomes following intravascular imaging-guided versus coronary angiography-guided percutaneous coronary intervention with stent implantation: a systematic review and Bayesian network meta-analysis of 31 studies and 17,882 patients. *JACC Cardiovasc Interv*. 2017;10:2488–2498. doi: [10.1016/j.jcin.2017.08.051](https://doi.org/10.1016/j.jcin.2017.08.051)
- Hong SJ, Mintz GS, Ahn CM, Kim JS, Kim BK, Ko YG, Kang TS, Kang WC, Kim YH, Hur SH, et al. Effect of intravascular ultrasound-guided drug-eluting stent implantation: 5-year follow-up of the IVUS-XPL randomized trial. *JACC Cardiovasc Interv*. 2020;13:62–71. doi: [10.1016/j.jcin.2019.09.033](https://doi.org/10.1016/j.jcin.2019.09.033)
- Lee JM, Choi KH, Song YB, Lee J-Y, Lee S-J, Lee SY, Kim SM, Yun KH, Cho JY, Kim CJ, et al. Intravascular imaging-guided or angiography-guided complex PCI. *N Engl J Med*. 2023;388:1668–1679. doi: [10.1056/NEJMoa2216607](https://doi.org/10.1056/NEJMoa2216607)
- Raber L, Mintz GS, Koskinas KC, Johnson TW, Holm NR, Onuma Y, Radu MD, Joner M, Yu B, Jia H, et al. Clinical use of intracoronary imaging. Part 1: guidance and optimization of coronary interventions. An expert consensus document of the European Association of Percutaneous Cardiovascular Interventions. *Eur Heart J*. 2018;39:3281–3300. doi: [10.1093/eurheartj/ehy285](https://doi.org/10.1093/eurheartj/ehy285)
- Prati F, Romagnoli E, Burzotta F, Limbruno U, Gatto L, La Manna A, Versaci F, Marco V, Di Vito L, Imola F, et al. Clinical impact of OCT findings during PCI: the CLI-OPCI II study. *JACC Cardiovasc Imaging*. 2015;8:1297–1305. doi: [10.1016/j.jcmg.2015.08.013](https://doi.org/10.1016/j.jcmg.2015.08.013)

10. Soeda T, Uemura S, Park SJ, Jang Y, Lee S, Cho JM, Kim SJ, Vergallo R, Minami Y, Ong DS, et al. Incidence and clinical significance of post-stent optical coherence tomography findings: one-year follow-up study from a multicenter registry. *Circulation*. 2015;132:1020–1029. doi: [10.1161/CIRCULATIONAHA.114.014704](https://doi.org/10.1161/CIRCULATIONAHA.114.014704)
11. Prati F, Romagnoli E, La Manna A, Burzotta F, Gatto L, Marco V, Fineschi M, Fabbiochi F, Versaci F, Trani C, et al. Long-term consequences of optical coherence tomography findings during percutaneous coronary intervention: the Centro Per La Lotta Contro L'infarto - Optimization Of Percutaneous Coronary Intervention (CLI-OPCI) LATE study. *EuroIntervention*. 2018;14:e443–e451. doi: [10.4244/EIJ-D-17-01111](https://doi.org/10.4244/EIJ-D-17-01111)
12. Rai H, Harzer F, Otsuka T, Abdelwahed YS, Antuna P, Blachutzik F, Koppa T, Raber L, Leistner DM, Alfonso F, et al. Stent optimization using optical coherence tomography and its prognostic implications after percutaneous coronary intervention. *J Am Heart Assoc*. 2022;11:e023493. doi: [10.1161/JAHA.121.023493](https://doi.org/10.1161/JAHA.121.023493)
13. Collet C, Sonck J, Vandeloof B, Mizukami T, Roosens B, Lochy S, Argacha JF, Schoors D, Colaiori I, Di Gioia G, et al. Measurement of hyperemic pullback pressure gradients to characterize patterns of coronary atherosclerosis. *J Am Coll Cardiol*. 2019;74:1772–1784. doi: [10.1016/j.jacc.2019.07.072](https://doi.org/10.1016/j.jacc.2019.07.072)
14. Sonck J, Nagumo S, Norgaard BL, Otake H, Ko B, Zhang J, Mizukami T, Maeng M, Andreini D, Takahashi Y, et al. Clinical validation of a virtual planner for coronary interventions based on coronary CT angiography. *JACC Cardiovasc Imaging*. 2022;15:1242–1255. doi: [10.1016/j.jcmg.2022.02.003](https://doi.org/10.1016/j.jcmg.2022.02.003)
15. Mizukami T, Sonck J, Sakai K, Ko B, Maeng M, Otake H, Koo B-K, Nagumo S, Norgaard BL, Leipsic J, et al. Procedural outcomes after percutaneous coronary interventions in focal and diffuse coronary artery disease. *J Am Heart Assoc*. 2022;11:e026960. doi: [10.1161/JAHA.122.026960](https://doi.org/10.1161/JAHA.122.026960)
16. Bulluck H, Paradies V, Barbato E, Baumbach A, Botker HE, Capodanno D, De Caterina R, Cavallini C, Davidson SM, Feldman DN, et al. Prognostically relevant periprocedural myocardial injury and infarction associated with percutaneous coronary interventions: a consensus document of the ESC Working Group on Cellular Biology of the Heart and European Association of Percutaneous Cardiovascular Interventions (EAPCI). *Eur Heart J*. 2021;42:2630–2642. doi: [10.1093/eurheartj/ehab271](https://doi.org/10.1093/eurheartj/ehab271)
17. Thygesen K, Alpert JS, Jaffe AS, Chaitman BR, Bax JJ, Morrow DA, White HD. Executive Group on behalf of the joint European Society of Cardiology/American College of Cardiology/American Heart Association / World Heart Federation Task Force for the Universal Definition of Myocardial I. Fourth Universal Definition of Myocardial Infarction (2018). *Circulation*. 2018;138:e618–e651. doi: [10.1161/CIR.0000000000000617](https://doi.org/10.1161/CIR.0000000000000617)
18. Araki M, Park SJ, Dauerman HL, Uemura S, Kim JS, Di Mario C, Johnson TW, Guagliumi G, Kastrati A, Joner M, et al. Optical coherence tomography in coronary atherosclerosis assessment and intervention. *Nat Rev Cardiol*. 2022;19:684–703. doi: [10.1038/s41569-022-00687-9](https://doi.org/10.1038/s41569-022-00687-9)
19. Hoshino M, Yonetsu T, Usui E, Kanaji Y, Ohya H, Sumino Y, Yamaguchi M, Hada M, Hamaya R, Kanno Y, et al. Clinical significance of the presence or absence of lipid-rich plaque underneath intact fibrous cap plaque in acute coronary syndrome. *J Am Heart Assoc*. 2019;8:e011820. doi: [10.1161/JAHA.118.011820](https://doi.org/10.1161/JAHA.118.011820)
20. Matsuo Y, Kubo T, Aoki H, Satogami K, Ino Y, Kitabata H, Taruya A, Nishiguchi T, Teraguchi I, Shimamura K, et al. Optimal threshold of postintervention minimum stent area to predict in-stent restenosis in small coronary arteries: an optical coherence tomography analysis. *Catheter Cardiovasc Interv*. 2016;87:E9–E14. doi: [10.1002/ccd.26143](https://doi.org/10.1002/ccd.26143)
21. Nakajima A, Araki M, Minami Y, Soeda T, Yonetsu T, McNulty I, Lee H, Nakamura S, Jang IK. Layered plaque characteristics and layer burden in acute coronary syndromes. *Am J Cardiol*. 2022;164:27–33. doi: [10.1016/j.amjcard.2021.10.026](https://doi.org/10.1016/j.amjcard.2021.10.026)
22. Radu MD, Raber L, Heo J, Gogas BD, Jorgensen E, Kelbaek H, Muramatsu T, Farooq V, Helqvist S, Garcia-Garcia HM, et al. Natural history of optical coherence tomography-detected non-flow-limiting edge dissections following drug-eluting stent implantation. *EuroIntervention*. 2014;9:1085–1094. doi: [10.4244/EIJV9I9A183](https://doi.org/10.4244/EIJV9I9A183)
23. Shimamura K, Kubo T, Akasaka T, Kozuma K, Kimura K, Kawamura M, Sumiyoshi T, Ino Y, Yoshizawa M, Sonoda S, et al. Outcomes of everolimus-eluting stent incomplete stent apposition: a serial optical coherence tomography analysis. *Eur Heart J Cardiovasc Imaging*. 2015;16:23–28. doi: [10.1093/ehjci/jeu174](https://doi.org/10.1093/ehjci/jeu174)
24. Sugiyama T, Yamamoto E, Fracassi F, Lee H, Yonetsu T, Kakuta T, Soeda T, Saito Y, Yan BP, Kurihara O, et al. Calcified plaques in patients with acute coronary syndromes. *JACC Cardiovasc Interv*. 2019;12:531–540. doi: [10.1016/j.jcin.2018.12.013](https://doi.org/10.1016/j.jcin.2018.12.013)
25. Tearney GJ, Regar E, Akasaka T, Adriaenssens T, Barlis P, Bezerra HG, Bouma B, Bruining N, Cho JM, Chowdhary S, et al. Consensus standards for acquisition, measurement, and reporting of intravascular optical coherence tomography studies: a report from the international working group for Intravascular Optical Coherence Tomography Standardization and Validation. *J Am Coll Cardiol*. 2012;59:1058–1072. doi: [10.1016/j.jacc.2011.09.079](https://doi.org/10.1016/j.jacc.2011.09.079)
26. Cook S, Eshtehardi P, Kalesan B, Raber L, Wenaweser P, Togni M, Moschovitis A, Vogel R, Seiler C, Eberli FR, et al. Impact of incomplete stent apposition on long-term clinical outcome after drug-eluting stent implantation. *Eur Heart J*. 2012;33:1334–1343. doi: [10.1093/eurheartj/ehr484](https://doi.org/10.1093/eurheartj/ehr484)
27. Chamie D, Bezerra HG, Attizzani GF, Yamamoto H, Kanaya T, Stefano GT, Fujino Y, Mehanna E, Wang W, Abdul-Aziz A, et al. Incidence, predictors, morphological characteristics, and clinical outcomes of stent edge dissections detected by optical coherence tomography. *JACC Cardiovasc Interv*. 2013;6:800–813. doi: [10.1016/j.jcin.2013.03.019](https://doi.org/10.1016/j.jcin.2013.03.019)
28. Kobayashi Y, Okura H, Kume T, Yamada R, Kobayashi Y, Fukuhara K, Koyama T, Nezu S, Neishi Y, Hayashida A, et al. Impact of target lesion coronary calcification on stent expansion. *Circ J*. 2014;78:2209–2214. doi: [10.1253/circj.cj-14-0108](https://doi.org/10.1253/circj.cj-14-0108)
29. Qiu F, Mintz GS, Witzenbichler B, Metzger DC, Rinaldi MJ, Duffy PL, Weisz G, Stuckey TD, Brodie BR, Parvataneni R, et al. Prevalence and clinical impact of tissue protrusion after stent implantation: an ADAPT-DES intravascular ultrasound substudy. *JACC Cardiovasc Interv*. 2016;9:1499–1507. doi: [10.1016/j.jcin.2016.05.043](https://doi.org/10.1016/j.jcin.2016.05.043)
30. Fujimura T, Matsumura M, Witzenbichler B, Metzger DC, Rinaldi MJ, Duffy PL, Weisz G, Stuckey TD, Ali ZA, Zhou Z, et al. Stent expansion indexes to predict clinical outcomes: an IVUS substudy from ADAPT-DES. *JACC Cardiovasc Interv*. 2021;14:1639–1650. doi: [10.1016/j.jcin.2021.05.019](https://doi.org/10.1016/j.jcin.2021.05.019)
31. Fujino A, Mintz GS, Matsumura M, Lee T, Kim SY, Hoshino M, Usui E, Yonetsu T, Haag ES, Shlofmitz RA, et al. A new optical coherence tomography-based calcium scoring system to predict stent under-expansion. *EuroIntervention*. 2018;13:e2182–e2189. doi: [10.4244/EIJ-D-17-00962](https://doi.org/10.4244/EIJ-D-17-00962)
32. Sanuki Y, Sonoda S, Muraoka Y, Shimizu A, Kitagawa M, Takami H, Anai R, Miyamoto T, Oginosawa Y, Tsuda Y, et al. Contribution of post-stent irregular protrusion to subsequent in-stent neoatherosclerosis after the second-generation drug-eluting stent implantation. *Int Heart J*. 2018;59:307–314. doi: [10.1536/ihj.17-463](https://doi.org/10.1536/ihj.17-463)
33. Bryniarski KL, Tahk SJ, Choi SY, Soeda T, Higuma T, Yamamoto E, Xing L, Dai J, Zanchin T, Lee H, et al. Clinical, angiographic, IVUS, and OCT predictors for irregular protrusion after coronary stenting. *EuroIntervention*. 2017;12:e2204–e2211. doi: [10.4244/EIJ-D-16-00679](https://doi.org/10.4244/EIJ-D-16-00679)
34. Sakai S, Sato A, Hoshi T, Hiraya D, Watabe H, Ieda M. In vivo evaluation of tissue protrusion by using optical coherence tomography and coronary angiography immediately after stent implantation. *Circ J*. 2020;84:2235–2243. doi: [10.1253/circj.CJ-20-0306](https://doi.org/10.1253/circj.CJ-20-0306)
35. Cook S, Wenaweser P, Togni M, Billinger M, Morger C, Seiler C, Vogel R, Hess O, Meier B, Windecker S. Incomplete stent apposition and very late stent thrombosis after drug-eluting stent implantation. *Circulation*. 2007;115:2426–2434. doi: [10.1161/CIRCULATIONAHA.106.658237](https://doi.org/10.1161/CIRCULATIONAHA.106.658237)
36. Foin N, Gutierrez-Chico JL, Nakatani S, Torii R, Bourantas CV, Sen S, Nijjer S, Petraco R, Kousera C, Ghione M, et al. Incomplete stent apposition causes high shear flow disturbances and delay in neointimal coverage as a function of strut to wall detachment distance: implications for the management of incomplete stent apposition. *Circ Cardiovasc Interv*. 2014;7:180–189. doi: [10.1161/CIRCINTERVENTIONS.113.000931](https://doi.org/10.1161/CIRCINTERVENTIONS.113.000931)
37. Wakabayashi H, Ando H, Nakano Y, Takashima H, Waseda K, Shimoda M, Ohashi H, Suzuki A, Sakurai S, Amano T. Temporal changes of incomplete stent apposition during early phase after everolimus-eluting stent implantation: serial optical coherence tomography analyses at 2-week and 4-month. *Int J Cardiovasc Imaging*. 2021;37:411–417. doi: [10.1007/s10554-020-02023-z](https://doi.org/10.1007/s10554-020-02023-z)
38. Munhoz D, Collet C, Mizukami T, Yong A, Leone AM, Eftekhari A, Ko B, da Costa BR, Berry C, Collison D, et al. Rationale and design of the Pullback Pressure Gradient (PPG) Global Registry. *Am Heart J*. 2023;265:170–179. doi: [10.1016/j.ahj.2023.07.016](https://doi.org/10.1016/j.ahj.2023.07.016)